current issues in molecular biology

MDPI

Article

Ethyl Acetate Extract of *Cynanchi Auriculati Radix* Inhibits LPS-Induced M1 Polarization of RAW264.7 Macrophages and Prolongs the Lifespan of *Caenorhabditis elegans* by Regulating NF-κB and PMK-1/SKN-1 Signaling Pathways

Jiawei Fan [1], Ya Su [1], Yi Xing [1], Kun Hu [1], Jie Ren [1,*] and Jia Yang [2,*]

[1] School of Pharmacy, Changzhou University, 21 Gehu Road, Changzhou 213164, China
[2] Purchasing and Supply Department, The Affiliated Changzhou No. 2 People's Hospital of Nanjing Medical University, NO. 68. Gehu Middle Road, Changzhou 213164, China
* Correspondence: renjie@cczu.edu.cn (J.R.); yangjia06150204@163.com (J.Y.)

Abstract

Extracts of *Cynanchi Auriculati Radix* (RCA), derived from the roots of *Cynanchum auriculatum* Royle ex Wight. (CA), have been documented to possess anti-inflammatory and antioxidant properties. However, the molecular mechanisms of their anti-aging action remain unclear. The present study aimed to explore the potential anti-aging components and mechanisms of RCA. LC-MS/MS and network pharmacology were used to identify components and targets. In vitro, LPS-induced RAW264.7 macrophages were used to assess anti-inflammatory effects. In vivo, *Caenorhabditis elegans* models were employed to evaluate lifespan and stress resistance. Five bioactive components were identified. The ethyl acetate extract of RCA (RCAEA) inhibited LPS-induced M1 macrophage polarization by suppressing the expression of NO, PGE2, IL-1β, iNOS, COX-2, TNF-α, and IL-6 via the NF-κB pathway. In *C. elegans*, RCAEA extended lifespan and enhanced oxidative and heat stress resistance, without affecting reproduction. These benefits were mediated by the PMK-1/SKN-1 pathway, as confirmed using mutant strains. RCAEA is a promising anti-aging and anti-inflammatory agent, acting through NF-κB and PMK-1/SKN-1 signaling pathways.

Keywords: *Cynanchum auriculatum* Royle ex Wight.; inflammation; aging; NF-κB; p38 MAPK; SKN-1; *Caenorhabditis elegans*

check for updates

Academic Editor: Anna Wai San Cheang

Received: 11 October 2025
Revised: 2 November 2025
Accepted: 6 November 2025
Published: 10 November 2025

Citation: Fan, J.; Su, Y.; Xing, Y.; Hu, K.; Ren, J.; Yang, J. Ethyl Acetate Extract of *Cynanchi Auriculati Radix* Inhibits LPS-Induced M1 Polarization of RAW264.7 Macrophages and Prolongs the Lifespan of *Caenorhabditis elegans* by Regulating NF-κB and PMK-1/SKN-1 Signaling Pathways. *Curr. Issues Mol. Biol.* **2025**, *47*, 934. https://doi.org/10.3390/cimb47110934

Copyright: © 2025 by the authors. Licensee MDPI, Basel, Switzerland. This article is an open access article distributed under the terms and conditions of the Creative Commons Attribution (CC BY) license (https://creativecommons.org/licenses/by/4.0/).

1. Introduction

Aging is an unstoppable natural process in which tissues and organs slowly lose their physiological functions. It often leads to related diseases, such as neurodegenerative diseases, immune dysfunction, and cancers, which have a profound impact on human health worldwide [1]. Aging is primarily driven by external stressors, and senescent cells enter a non-dividing state triggered by many factors, including deoxyribonucleic acid (DNA) damage [2], oxidative stress, and chromatin structure changes, leading to accelerated organ and cell degeneration [3]. Inflammation, a chronic and progressive state that accompanies the aging process, is characterized by chronically elevated cytokine levels [4]. At present, anti-inflammatory therapies have been shown to alleviate aging-related diseases and extend lifespan [5]. Therefore, identifying new therapeutic targets and interventions to reduce various aging-related diseases caused by inflammation is important.

Currently, many extracts from natural plants have been demonstrated to possess anti-aging effects [6,7]. To systematically investigate their underlying therapeutic mechanisms [8], advanced bioinformatics tools like network pharmacology (NP) were utilized in the modern pharmacology area [9]. NP can enhance scientific rigor and application value [10,11], thus facilitating the discovery of novel drug targets and molecular pathways and ultimately clarifying drug actions from the perspective of multi-dimensional biological networks [12].

Cynanchum auriculatum Royle ex Wight. (CA), commonly known as "Baishouwu" in China, can be converted into tea and starch for food industry use [13]. To date, 151 pure compounds have been identified in *Cynanchi Auriculati Radix* (RCA) and categorized into C_{21}-steroids, acetophenones, flavonoids, alkaloids, and terpenoids. C_{21}-steroids demonstrate strong anti-tumor activity [14,15]. Furthermore, acetophenones and crude extracts have exhibited immunomodulatory, anti-inflammatory, and antidepressant properties. Other investigations have also revealed that their chemical compositions have considerable medicinal value [16,17]. In contrast, the anti-aging impact of RCA by regulating inflammation-related factors and signaling pathways remains largely unexplored.

Therefore, we hypothesize that the ethyl acetate extract of RCA (RCAEA), for which its chemical components have been identified by liquid chromatography–tandem mass spectrometry (LC-MS/MS), can exert protective effects by reducing lipopolysaccharide (LPS)-induced inflammatory damage in RAW264.7 macrophages through the regulation of inflammatory mediators and macrophage polarization parameters. Subsequently, we assume that RCAEA can demonstrate anti-aging effects by influencing longevity-related biomarkers of *C. elegans* and that its underlying molecular mechanisms can be elucidated. Collectively, these assumed effects and mechanisms are expected to offer new insights into the protective mechanisms of RCAEA in aging processes.

2. Materials and Methods

2.1. Materials and Reagents

The plant material was harvested from Binhai County, Jiangsu Province, China, in December 2020 and stored in a shaded location for later use. It was identified as RCA by Prof. Jie Ren from Changzhou University, China. Analytical-grade ethanol, petroleum ether, methylene chloride, ethyl acetate, and n-butanol were purchased from Energy Chemistry (Shanghai, China). Trypsin, Arc-Bis, Trisma Base, and Glycine were purchased from Biosharp (Guangzhou, China). The Methyl Thiazolyl Tetrazolium (MTT) Kit, Griess Kit, and Enzyme-Linked Immunosorbent Assay (ELISA) Kit were purchased from Qiao Yi Biotechnology, Co., Ltd. (Hefei, China). Radio Immunoprecipitation Assay (RIPA) Lysate and a BCA Test Kit were purchased from KGI Biotechnology, Co., Ltd. (Nanjing, China). All antibodies were from Beyotime (Shanghai, China). The Ultra-Pure Total RNA Rapid Extraction Kit was from Genenode (Wuhan, China), and the ECL Western Blotting Substrate was from Proteintech (Chicago, IL, USA). Primers for qPCR were synthesized by GenScript Biotech (Nanjing, China). The nuclear and cytoplasmic protein extraction kit (P0028) was purchased from Beyotime (Shanghai, China).

2.2. The Preparation for RCAEA

As reported by Su et al. [18], RCAEA was prepared. The extraction and separation flowchart is shown in Figure S1.

2.3. LC-MS/MS Instrumentation and Conditions

LC-MS/MS analysis was conducted on an AB SCIEX Instruments 6600 Triple TOF (Applied Biosystems, Foster City, CA, USA) coupled with Prominence-I LC-2030C 3D

HPLC system (Shimadzu, Kyoto, Japan). The specific experimental conditions are detailed in the Supplementary Materials.

2.4. Network Aharmacology Analysis

Based on the results of LC-MS/MS, the Traditional Chinese Medicine Systems Pharmacology (TCMSP) platform (https://www.tcmsp-e.com/, accessed on 8 August 2025), the PubChem platform (https://pubchem.ncbi.nlm.nih.gov, accessed on 8 August 2025), and the Swiss Target Prediction databases (https://www.swisstargetprediction.ch/, accessed on 8 August 2025) were chosen to obtain the active components targets of RCAEA. The UniProt database (http://www.uniprot.org, accessed on 8 August 2025) was used to standardize gene symbol names. The human gene targets of aging were identified in the GeneCards database (https://www.genecards.org/, accessed on 8 August 2025), OMIM database (https://www.omim.org/, accessed on 8 August 2025), DisGeNET database (https://www.disgenet.org/, accessed on 8 August 2025), and DrugBank database (https://www.drugbank.ca/, accessed on 8 August 2025). The Venny 2.1.0 platform (https://bioinfogp.cnb.csic.es/tools/venny/, accessed on 8 August 2025) was used to screen the common targets of drugs and diseases. Then, the String database (https://string-db.org, accessed on 8 August 2025) and Cytoscape 3.10.0 software were utilized to select the critical targets. Finally, the enrichment analyses of Gene Ontology (GO) functions and the Kyoto Encyclopedia of Genes and Genomes (KEGG) were performed using the STRING online platform (https://string-db.org, accessed on 8 August 2025), and Cytoscape 3.10.1 software was employed to create a network diagram of drug–target–pathway–disease interactions.

2.5. Cell Culture and Viability Assays

RAW264.7 macrophage cells (ZQ0098) were provided by Zhong Qiao Xin Zhou Biotechnology Co., Ltd. (Shanghai, China). LPS (L6529-1 mg) was purchased from Sigma-Aldrich (Shanghai, China). The cells were cultured in Dulbecco's Modified Eagle Medium (DMEM), which contained 10% FBS, 100 U/mL penicillin, and 100 μg/mL streptomycin at 37 °C in a humidified atmosphere of 5% CO_2. The toxicity of RCAEA (25, 50, 100, 200, 400, and 800 μg/mL) and LPS (100, 200, 400, and 800 ng/mL) was detected according to the absorbance values at 570 nm by the MTT method to determine the concentration to be used for subsequent experiments [19]. Then, cells were treated with RCAEA (25, 50, and 100 μg/mL) and LPS (200 ng/mL). LPS (200 ng/mL) was used for the induction of M1 polarization for 24 h. Nitric oxide (NO) concentrations were measured using the Griess Kit according to the manufacturer's instructions [20].

2.6. ELISA

RAW264.7 cells were treated with RCAEA (25, 50, and 100 μg/mL) or 200 ng/mL LPS for 24 h. Then, the cell supernatant was collected. We carried out the subsequent operations in accordance with the instructions of the ELISA kits (Jianglai Biotechnology Co., LTD., Shanghai, China) [21]. The details are in the Supplementary Materials.

2.7. Real-Time Quantitative PCR (qRT-PCR) Assay of RAW264.7 Cells

RAW264.7 macrophages were treated with RCAEA (25, 50, 100 μg/mL) in the presence or absence of LPS (200 ng/mL). Each treatment condition, including different concentrations of RCAEA and LPS, was added in duplicate to a 24-well plate (100 μL per well). Following treatment, the total RNA was extracted using an Ultra-Pure Total RNA Rapid Extraction Kit. Then, cDNA was synthesized by reverse transcription. The *β-actin* gene was used as an internal control. mRNA expression levels of targeted genes were quantified using the

$2^{-\Delta\Delta Ct}$ method. The primer sequences and experimental conditions of genes are listed in Tables S1 and S2.

2.8. Western Blotting

The method was carried out according to [22,23]. The following primary antibodies were used: β-actin (1:2000), Lamin B (1:2000), inducible nitric oxide synthase (iNOS) (1:5000), cyclooxygenase-2 (COX-2) (1:5000), nuclear factor kappa-B (NF-κB) (1:2000), IκBα (1:5000), and p-IκBα (1:5000). Bands were visualized using a Tanon 5200 imaging system (Tanon, Shanghai, China). The protein expressions were quantified using ImageJ 1.8.0 software (National Institutes of Health, Bethesda, MD, USA).

2.9. Immunofluorescence

RAW264.7 cells were cultured in 12-well plates and subjected to the indicated treatments for 24 h. The details are presented in the Supplementary Materials.

2.10. Cultivation and Synchronization of Caenorhabditis Elegans (C. elegans)

N2, Bristol wild-type; EU1, *skn-1(zu67) IV/nT1 [unc-?(n754) let-?] (IV;V)*; KU4, *sek-1 (km 4)X* and KU25, *pmk-1(km25) IV*. These strains were sourced from the Caenorhabditis Genetics Center (CGC).

C. elegans were cultured on nematode growth medium (NGM), with *Escherichia coli* (*E. coli*) OP50 [22]. After repeatedly rinsing the worms with 1 mL of M9 buffer, they were placed in sterile 1.5 mL EP tubes. Then, 750 µL of lysis buffer was added, and the samples were vortexed for 5 min and centrifuged at 4000 rpm for 2 min. After removing the supernatant, the pellet was washed by adding 1 mL of M9 buffer for rinsing. This washing and centrifugation step was repeated twice. The collected eggs were then transferred onto fresh NGM and incubated at 20 °C until the progeny reached the L4 stage, completing the synchronization process.

2.11. Bacterial Growth Rates

As referenced in [24], the experimental conditions were adjusted. The detailed experimental conditions can be found in the Supplementary Materials.

2.12. Locomotor Behavior Assays

The synchronized L4-staged worms were cultured on NGM treated with or without RCAEA (0.25, 0.5, 1, 2, 4, 8, and 16 mg/mL) at 20 °C for 4 days to assess their motility. For each group, at least five worms were randomly selected. The number of head wiggles made by the worms in each group within 30 s was measured, with a head wiggle from one side to the other side counted as once [25].

2.13. Lifespan Assay

At least fifty synchronized L4-staged worms were randomly selected from each group and cultured on NGM treated with or without RCAEA (1, 2, and 4 mg/mL) at 20 °C. The daily survival of the worms was monitored by transferring surviving worms to fresh NGM until all died. Death was confirmed by the lack of response of the worms to platinum wire stimulation at both the head and tail. Survival rates were calculated, and survival curves were generated [26].

2.14. Reproduction Assay

At least five *C. elegans* were cultured as described in Section 2.13. Subsequently, the number of eggs produced was recorded every 24 h for 5 consecutive days [27].

2.15. Stress Assay

At least ten *C. elegans* were cultured as described in Section 2.13 for 48 h.

Oxidative Stress: Worms were transferred to NGM containing 50 μM juglone. The number of surviving worms was counted every 0.5 h until all died. Worms were considered dead when they did not react to a light touch. Survival rates were calculated, and survival curves were generated.

Heat Stress: At least fifteen worms were randomly selected and placed onto a new NGM in a constant-temperature incubator at 35 °C. The number of dead worms, surviving worms, and total worms was counted every 1 h. Survival rates were calculated, and survival curves were generated.

2.16. Measurement of Reactive Oxygen Species (ROS)

C. elegans were cultured as described in Section 2.13 for 3 days. These worms were exposed to 50 mM H_2O_2 for 4 h [28]. The specific experimental protocol is presented in the Supplementary Materials.

2.17. Lipofuscin Assays

C. elegans were cultured as described in Section 2.13 for 12 days. After spawning, at least five worms from each group were randomly selected and anesthetized with 0.1% NaN_3. The spontaneous fluorescence of lipofuscin in the worms was observed and photographed at 100× magnification [29]. The lipofuscin accumulation level was quantified based on fluorescence intensity using ImageJ software.

2.18. qRT-PCR of C. Elegans

The total RNA of worms was extracted by Hu et al. [30], and reverse transcription was performed following the instructions of the corresponding kit. Three replicate wells were set for each sample. The *β-actin* gene was used as an internal control. The primer sequences and conditions for each gene are listed in Tables S1 and S3.

2.19. Data Analysis

All experiments were performed in triplicate. Statistical analyses were conducted using GraphPad Prism 9 software (GraphPad Software, San Diego, CA, USA). Data were presented as the mean ± standard deviation (SD). For multiple group comparisons, one-way or two-way ANOVA was employed, followed by an appropriate post hoc test. For comparisons between two groups, Student's *t*-test was used. Survival data were analyzed by the Kaplan–Meier method, and the log-rank test was applied for curve comparisons. The mean lifespan was calculated from three independent experiments, with the standard error of the mean (SEM) derived from these replicates. $p < 0.05$ was considered to be statistically significant.

3. Results

3.1. Qualitative Analysis of the Components in RCAEA by LC-MS/MS

In total, 0.93 g of the ethyl acetate extract was obtained from the fresh roots of RCA samples (100 g). The compounds of RCAEA are shown in Figure 1. Five constituents were tentatively identified based on retention times, formulas, and error values (Table 1). The published literature provided some useful information for the identification of compound structures [16,17].

Table 1. Chemical profiling of major ingredients in RCAEA.

t_R	Compound Name	Formula	Precursor *m/z*	Reference *m/z*	Error (ppm)	Mode
11.669	Caudatin	$C_{28}H_{42}O_7$	491.29912	491.29999	−1.77	$[M+H]^+$
16.415	Beta-Sitosterol	$C_{29}H_{50}O$	397.38257	397.38287	−0.75	$[M+H]^+$
6.741	Baishouwubenzophenone	$C_{16}H_{14}O_6$	301.0731	301.0744	4.4	$[M-H]^-$
5.994	4′-Hydroxyacetophenone	$C_8H_8O_2$	135.0456	135.0460	3.3	$[M-H]^-$
13.714	2,4-Dihydroxyacetophenone	$C_8H_8O_3$	151.0400	151.0399	−0.4	$[M+H]^+$

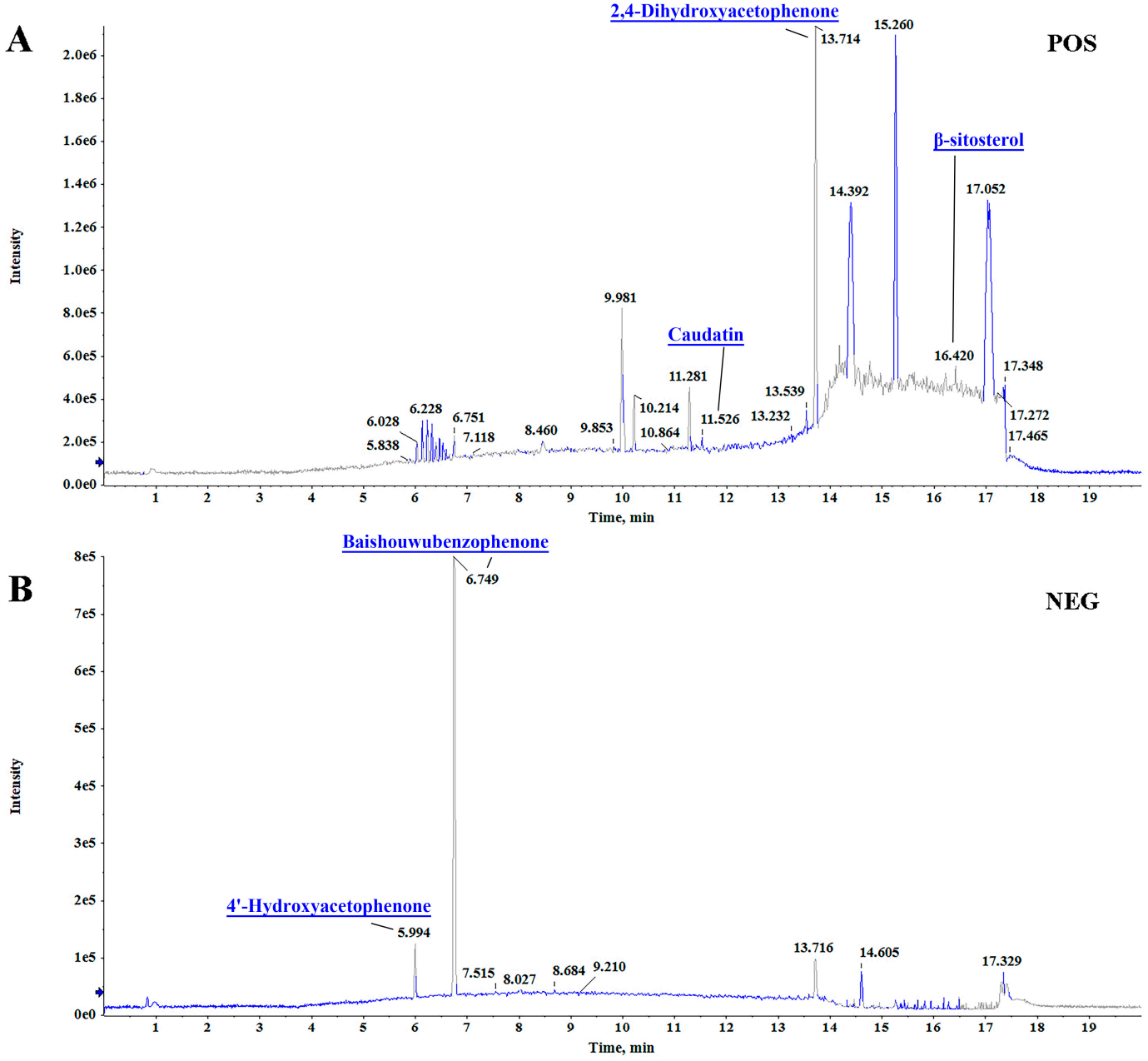


Figure 1. Qualitative analysis of the chemical components in RCAEA. Total ion chromatograms of RCAEA in the positive ion mode (**A**) and negative ion mode (**B**).

3.2. Predict the Anti-Aging Mechanism of RCAEA by Network Pharmacology Analysis

According to the process shown in Figure 2A, after importing the active ingredients of RCAEA into SwissTargetPrediction, 334 corresponding targets were obtained. Then, 5351 potential disease targets were identified from four disease databases. Intersection

analyses revealed 242 candidate anti-aging targets of RCAEA (Figure 2B). The protein–protein interaction (PPI) of the core target interaction map showed that AKT1, SRC, EGFR, and TNF had higher node degrees (Figure 2C). Then, KEGG pathways were determined through enrichment analysis, including the regulation of the mitogen-activated protein kinase (MAPK) signaling pathway and the NF-kappa B signaling pathway (Figure 2D). GO analyses indicated that the biological process (BP) mainly involved inflammatory responses. Cellular components (CCs) mainly included the plasma membrane. Molecular functions (MFs) mainly included nuclear receptor activity (Figure 2E). This fully demonstrates that RCAEA improves aging through diverse biological mechanisms that regulate cellular and molecular functions.

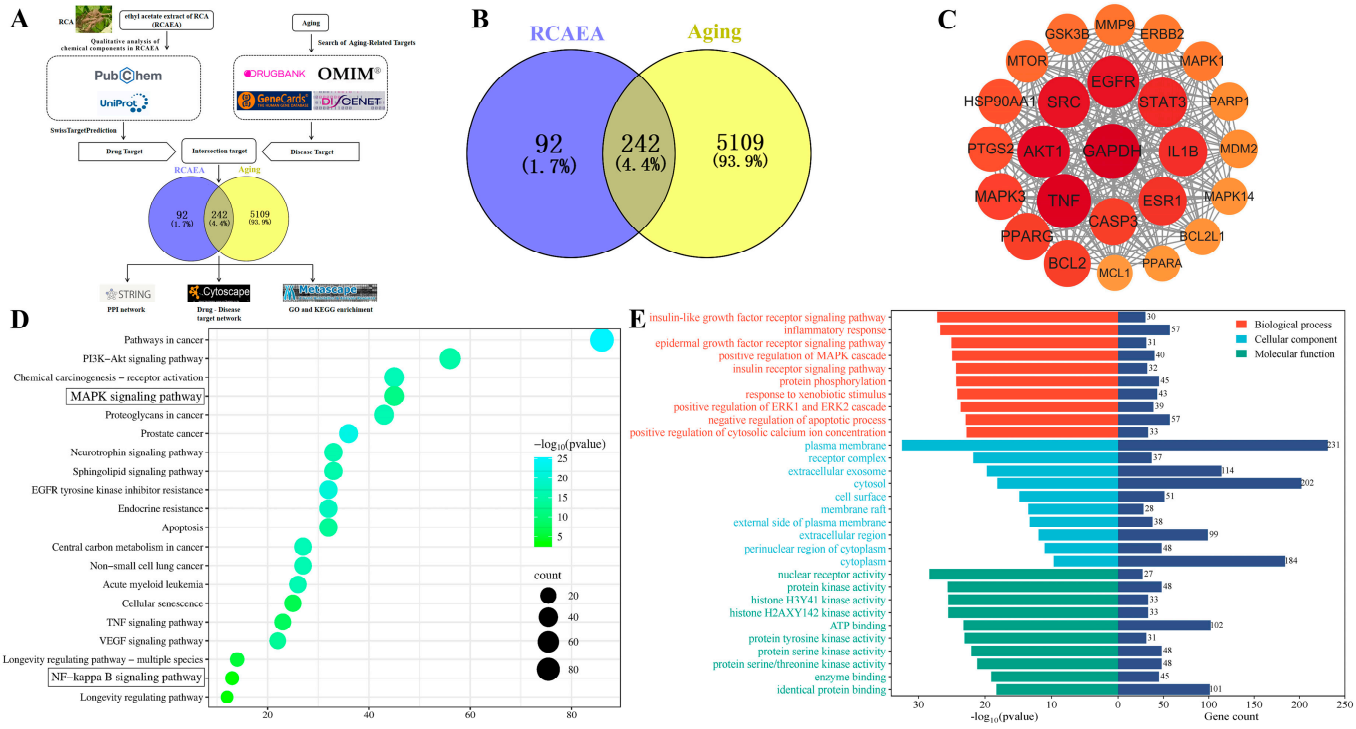


Figure 2. Network pharmacology revealed the key anti-aging mechanisms of RCAEA. (**A**) Process of network pharmacology analysis. (**B**) Venn diagram showing the overlap between RCAEA and aging. (**C**) PPI network of core targets. (**D**) KEGG pathway enrichment analysis of RCAEA. (**E**) GO functional enrichment analysis of RCAEA.

3.3. RCAEA Suppresses M1-Type Polarization in RAW264.7 Macrophages Under Inflammatory Environment

Firstly, cell viability assays confirmed that neither RCAEA (25, 50, and 100 μg/mL) nor LPS (100 and 200 ng/mL) significantly affected cell survival (Figure 3A,B). The LPS treatment (100, 200, 400, and 800 ng/mL) promoted macrophage polarization into the M1-type, characterized by increased production levels of NO (Figure 3C) [31]. In total, 200 ng/mL of LPS was finally chosen for further experiments based on cytotoxicity assessment. RCAEA samples measuring 25, 50, and 100 μg/mL notably inhibited the LPS (200 ng/mL)-induced production of NO (Figure 3D) and improved cell viability (Figure 3E). These concentrations were selected for subsequent experiments.

Excessive iNOS expression and NO production are key markers of the inflammatory response. RCAEA downregulated the expression of iNOS at both the protein and mRNA levels (Figure 3G,I). Similarly, RCAEA inhibited the production of COX-2 and PGE2 (Figure 3F,H,I). It also reduced the mRNA levels of tumor necrosis factor-alpha (TNF-α),

interleukin-6 (IL-6), and IL-1β (Figure 3I). Taken together, RCAEA exhibited significant inhibitory activity against inflammation.

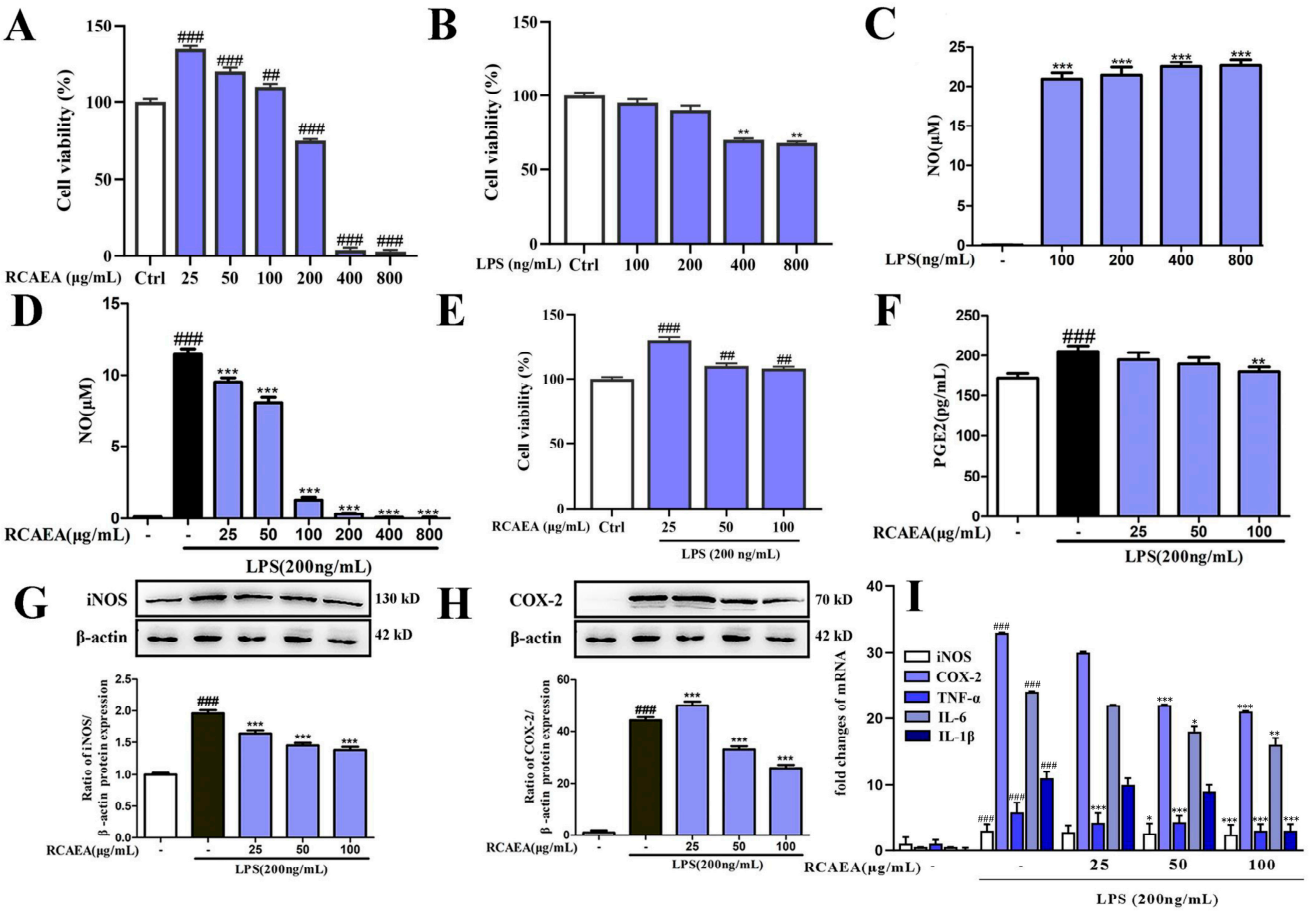


Figure 3. RCAEA reduces the production of inflammatory factors in LPS-induced RAW264.7 cells. (**A**) Cytotoxicity of RCAEA in RAW264.7 cells. (**B**) Cytotoxicity of LPS in RAW264.7 cells. (**C**) The release level of NO in RAW264.7 cells treated with LPS. (**D**) The release level of NO in LPS-induced RAW264.7 cells treated with RCAEA. (**E**) Cytotoxicity in LPS-induced RAW 264.7 cells treated with RCAEA. (**F**) The PGE2 level in LPS-induced RAW264.7 macrophages. (**G**,**H**) Effects of RCAEA on iNOS and COX-2 expression levels at the protein level. *β-actin* was used as the internal control for normalization. (**I**) The mRNA levels of inflammation factors. Values = mean ± SD, $n = 3$ (* $p < 0.05$, ** $p < 0.01$, and *** $p < 0.001$ compared to the LPS-treated group; $^{\#\#}$ $p < 0.01$ and $^{\#\#\#}$ $p < 0.001$ compared to the control group).

3.4. RCAEA Blocks NF-κB Pro-Inflammatory Signaling Pathway

Inflammation is related to the regulation of the NF-κB signaling pathway [32]. The results suggest that NF-κB was transferred from the cytoplasm to the nucleus, and the protein expression of NF-κB was increased in the nucleus in LPS-treated RAW264.7 macrophages (Figure 4A,C). Meanwhile, the protein expression level of the phosphorylated NF-κB inhibitor α (IκBα) decreased after RCAEA treatment (Figure 4B), which reduced the nuclear transfer capacity of NF-κB and thus decreased the production of inflammatory cytokines [33]. The data suggest that RCAEA might regulate the expression of inflammatory cytokines to inhibit macrophage polarization via the NF-kB signaling pathway.

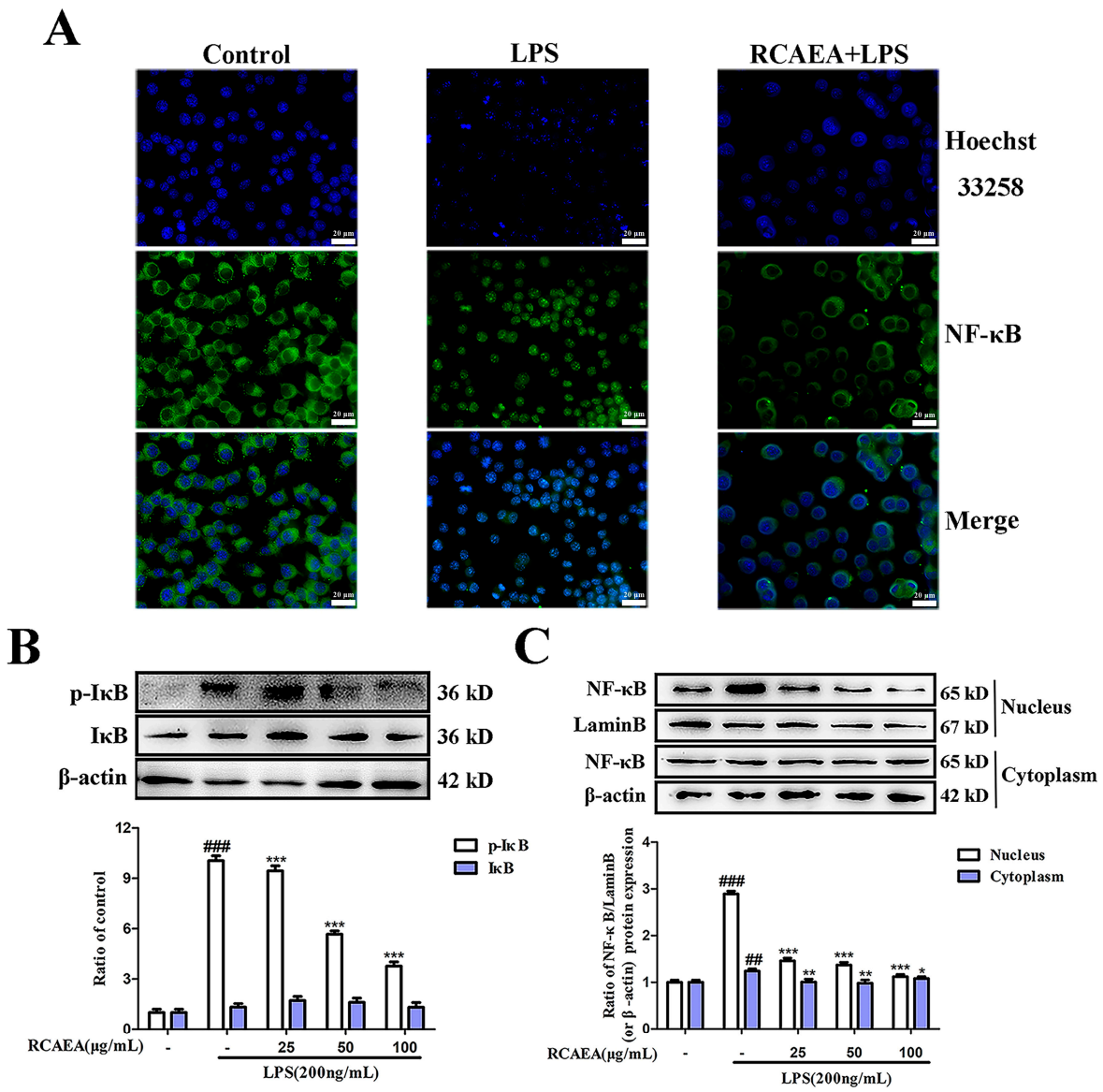


Figure 4. RCAEA modulated macrophage polarization and reduced the production of inflammatory factors in LPS-induced RAW264.7 cells via the NF-κB signaling pathway. (**A**) Localization images of NF-κB p65 in RAW264.7 cells. (**B**) Effects of RCAEA on LPS-induced IκBα phosphorylation. (**C**) Effects of RCAEA on LPS-induced NF-κB activation. *Lamin B* and *β-actin* were used as internal parameters for normalization. Values = mean ± SD, $n = 3$ (* $p < 0.05$, ** $p < 0.01$, and *** $p < 0.001$ compared to the LPS-treated group; $^{\#\#}$ $p < 0.01$ and $^{\#\#\#}$ $p < 0.001$ compared to the control group).

3.5. The Influence of RCAEA on the Biological Behaviors and Aging Process of C. elegans

As shown in Figure 5A, RCAEA exhibited no anti-bacterial activity against *E. coli* OP50, confirming that subsequent effects on *C. elegans* were not due to microbial growth inhibition. As *C. elegans* age, their head-swinging frequency gradually declines until they ultimately die [34]. High doses of RCAEA (8 and 16 mg/mL) may have had toxic effects on N2 *C. elegans*, while low doses of RCAEA (0.25 and 0.5 mg/mL) had no significant influence on *C. elegans*. Therefore, 1, 2, and 4 mg/mL were selected for further analysis. RCAEA-treated (1, 2, 4 mg/mL) worms showed significantly higher head wiggle frequencies than controls (Figure 5B). This indicated that RCAEA improved the locomotor function of worms. The egg-laying number also reflected that RCAEA had no reproductive toxicity (Figure 5C,D).

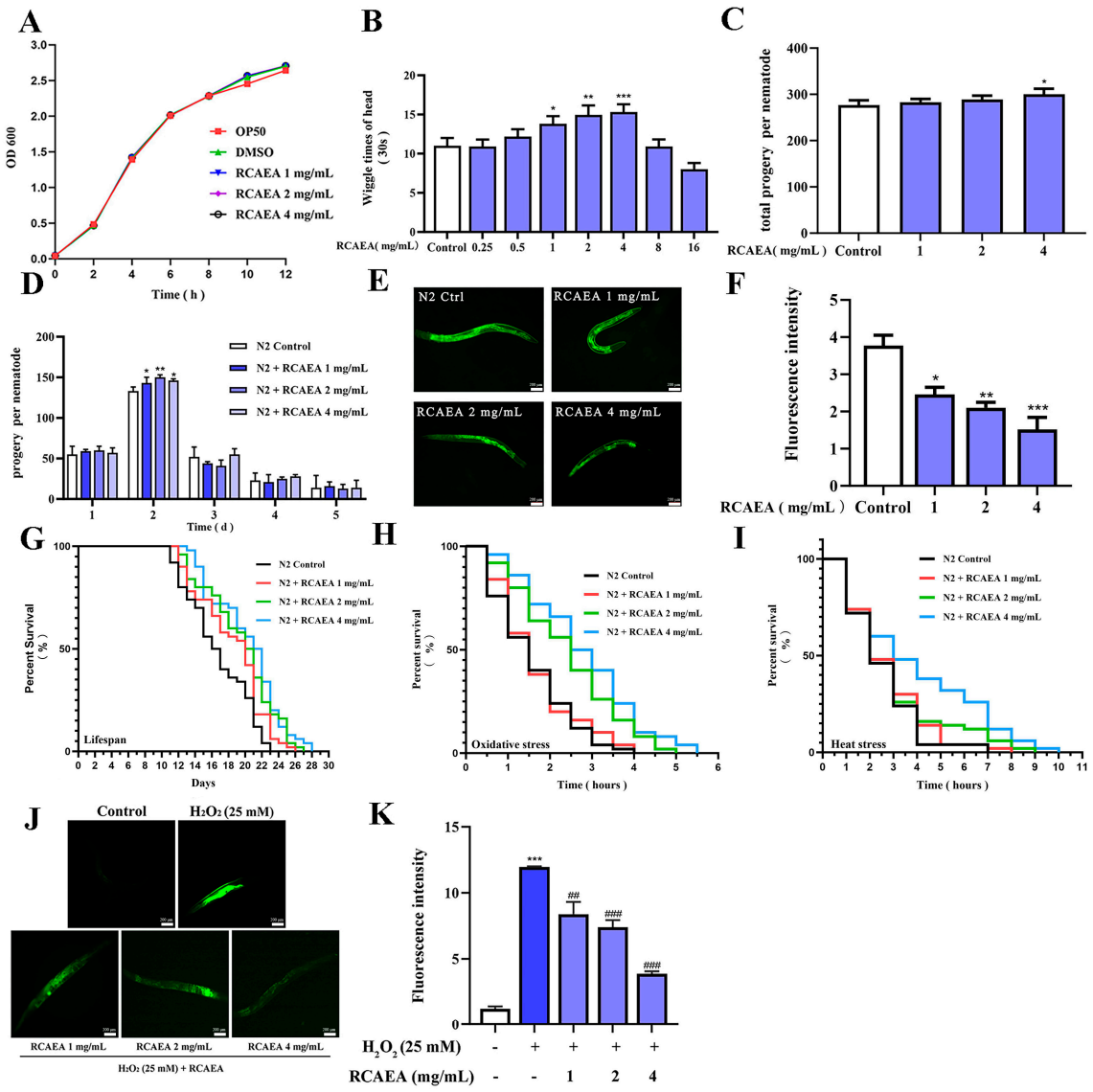


Figure 5. RCAEA improves biological behaviors and longevity in N2 *C. elegans*. (**A**) Effect of RCAEA on the growth rate of *E. coli* OP50. (**B**) RCAEA showed no toxicity in *C. elegans* (n = 30). (**C**,**D**) RCAEA showed no reproductive toxicity on N2 *C. elegans* (n = 5). (**E**,**F**) RCAEA reduces lipofuscin accumulation in N2 *C. elegans*. Lipofuscin accumulation was quantified using ImageJ software (n = 50). (**G**) RCAEA extended the lifespan of N2 *C. elegans* (n = 50, log-rank test). (**H**,**I**) RCAEA protected *C. elegans* from the damage induced by juglone and 35 °C heat (n = 50, log-rank test). (**J**,**K**) RCAEA reduced the ROS level induced by H_2O_2 (n = 50). Values = mean ± SD, n = 3 (* $p < 0.05$, ** $p < 0.01$, and *** $p < 0.001$ compared to the control group; $^{\#\#}$ $p < 0.01$ and $^{\#\#\#}$ $p < 0.001$ compared to the H_2O_2-treated group).

The RCAEA treatment group significantly reduced lipofuscin accumulation, a quantitative biomarker of cellular aging [35]. This was evidenced by markedly weaker lipofuscin, which was 59.79% lower in the high-dose RCAEA group (4 mg/mL) compared to controls (Figure 5E,F) [36]. Juglone, a substance known to generate significant levels of superoxide radicals, and heating, which will lead to physiological changes, were observed. They all induce oxidative stress and reduce nematode viability [37,38]. RCAEA not only extended the lifespan of N2 worms (Figure 5G and Table 2) but also significantly increased the anti-stress capacity to prolong the maximum lifespan under juglone and heat stress compared to the controls (Figure 5H,I and Table S4). The excellent antioxidant capacity of RCAEA was also demonstrated by detecting ROS levels using the DCF-DA fluorescent

probe, a well-established ROS-sensitive dye [39]. H_2O_2 could elevate ROS levels in *C. elegans* through externally induced oxidative stress [40]. Compared with the H_2O_2 group, RCAEA treatment at 4 mg/mL resulted in the lowest fluorescence intensity (Figure 5J,K). Based on the above experiments, it can be inferred that RCAEA may promote longevity via improving biological characteristics and anti-stress capacity in *C. elegans* [41].

Table 2. The effects of RCAEA on the lifespan of N2 *C. elegans*.

Sample	Median Lifespan/d	Max Lifespan/d	Increase in Average Lifespan/%	*p*-Value vs. Control
Control	16.33 ± 0.17	22.33 ± 0.67	-	-
1 mg/mL RCAEA	20.22 ± 0.22	26.00 ± 0.00	16.42	0.0027 **
2 mg/mL RCAEA	20.50 ± 0.29	26.33 ± 0.33	17.91	0.0029 **
4 mg/mL RCAEA	21.33 ± 0.17	27.67 ± 0.33	23.88	0.0010 ***

Data are expressed as the mean ± SEM (n = 3); ** $p < 0.01$, and *** $p < 0.001$.

3.6. RCAEA Prolongs the Lifespan of C. elegans via the PMK-1/SKN-1 Signaling Pathway

Based on the core targets identified in the PPI analysis, we analyzed the expression of aging-associated genes, such as *src*, *let-23*, *trf-2*, and *akt-1* in N2 *C. elegans*. They all played certain roles in the aging process (Figure 6A). Notably, RCAEA treatment significantly increased the expression levels of *skn-1*-associated genes, such as *skn-1*, *sod-1*, *sod-3*, and *gst-4* (Figure 6B). Since *skn-1* is a primary regulator of the p38 MAPK/PMK-1 pathway [42], the effects of RCAEA are likely to involve the regulation of the *skn-1*-mediated *pmk-1*.

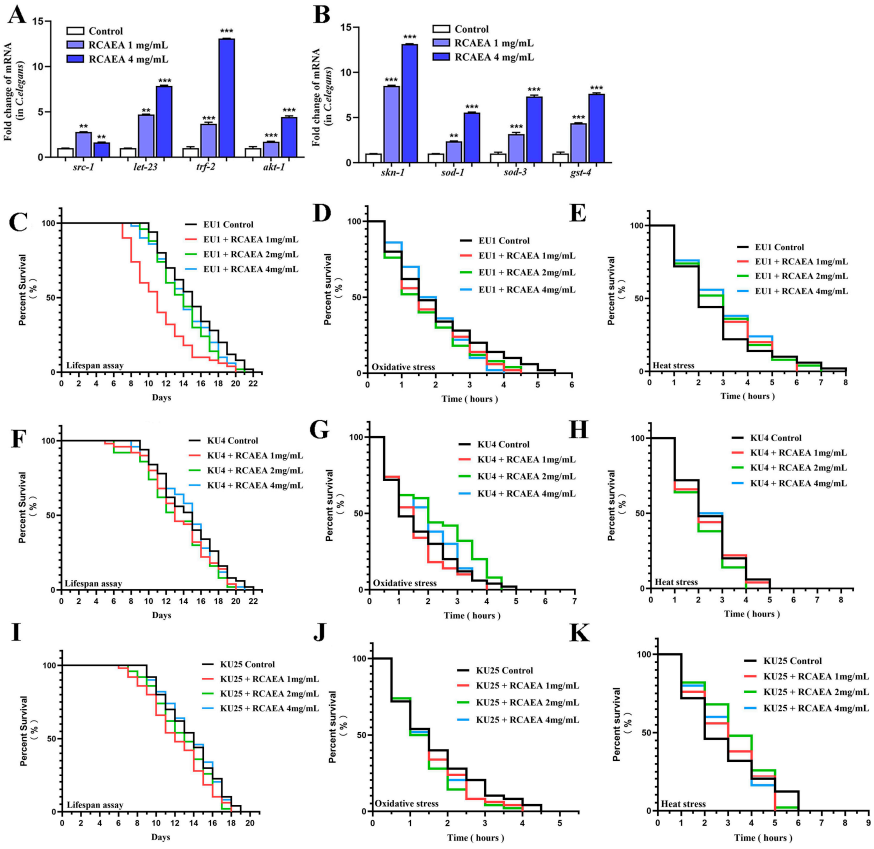


Figure 6. RCAEA extends the lifespan of *C. elegans* through PMK-1/SKN-1 signaling pathway. (**A**) Effects of RCAEA on anti-aging genes predicted by PPI. (**B**) RCAEA enhances the expression levels of antioxidant-related genes. (**C**–**K**) RCAEA mediates the longevity of *C. elegans* via PMK-1/SKN-1 signaling pathway (n = 50, log-rank test). Values = mean ± SD, n = 3 (** $p < 0.01$ and *** $p < 0.001$ compared to the control group).

To further explore whether RCAEA enhances anti-aging abilities through the PMK-1/SKN-1 signaling pathway, we conducted stress and lifespan assays in the EU1, KU4, and KU25 mutants. As shown in Figure 6C–K, Tables 3–5, and Tables S5–S7, when *skn-1*, *sek-1*, and *pmk-1* were deficient, RCAEA did not extend the resistance to stress and lifespan under normal and stressful conditions [43]. Collectively, these findings indicate that the RCAEA may influence stress resistance and lifespan extension via the PMK-1/SKN-1 pathway in *C. elegans*.

Table 3. The effects of RCAEA on the lifespan of the EU1 mutant.

Sample	Median Lifespan/d	Max Lifespan/d	Increase in Average Lifespan/%	*p*-Value vs. Control
Control	14.67 ± 0.33	21.67 ± 0.33	-	-
1 mg/mL RCAEA	11.67 ± 0.33	20.33 ± 0.33	−6.15	ns
2 mg/mL RCAEA	13.67 ± 0.33	20.67 ± 0.33	−4.62	ns
4 mg/mL RCAEA	14.00 ± 0.00	20.67 ± 0.33	−4.62	ns

Data are expressed as the mean ± SEM (n = 3); ns = not significant.

Table 4. The effects of RCAEA on the lifespan of the KU4 mutant.

Sample	Median Lifespan/d	Max Lifespan/d	Increase in Average Lifespan/%	*p*-Value vs. Control
Control	14.67 ± 0.33	21.67 ± 0.33	-	-
1 mg/mL RCAEA	12.67 ± 0.33	20.33 ± 0.33	−6.15	ns
2 mg/mL RCAEA	13.00 ± 0.00	21.00 ± 0.58	−3.08	ns
4 mg/mL RCAEA	14.33 ± 0.33	20.67 ± 0.33	−4.62	ns

Data are expressed as the mean ± SEM (n = 3); ns = not significant.

Table 5. The effects of RCAEA on the lifespan of the KU25 mutant.

Sample	Median Lifespan/d	Max Lifespan/d	Increase in Average Lifespan/%	*p*-Value vs. Control
Control	13.67 ± 0.33	18.67 ± 0.33	-	-
1 mg/mL RCAEA	11.33 ± 0.33	17.67 ± 0.33	−5.36	ns
2 mg/mL RCAEA	13.00 ± 0.58	17.00 ± 0.58	−8.93	ns
4 mg/mL RCAEA	12.67 ± 0.67	17.33 ± 0.33	−7.14	ns

Data are expressed as the mean ± SEM (n = 3); ns = not significant.

4. Discussion

During aging, the underlying proinflammatory state increases and leads to inflammatory phenomena. Macrophages undergo phenotypic adaptations in response to stimuli, such as LPS, which is typically characterized by polarization into the M1 phenotype with the robust secretion of inflammatory mediators. These inflammatory mediators may undergo mutual regulation and are mediated by each other [44]. The regulation of macrophage phenotype is important for inflammation prevention [45]. Therefore, RAW264.7 macrophages were chosen as a suitable model for the in vitro experiment [46].

RAW264.7 macrophages can polarize to the M1 phenotype by LPS, as confirmed by our research on characteristic markers, such as NO, iNOS, and COX-2. iNOS catalyzes sustained, high-output NO production, while COX-2 converts arachidonic acid into its principal bioactive product. Under physiological conditions, iNOS and COX-2 are expressed at low levels. However, their expression levels are markedly upregulated in response to inflammatory factor stimuli [47–49]. Here, we demonstrated that RCAEA exerts significantly anti-inflammatory effects in LPS-induced RAW264.7 cells. The NF-κB signaling pathway

serves as a key target for modulating inflammatory responses, and its activity directly affects iNOS and COX-2. Under the stimulation of an inflammatory environment, phosphorylated NF-κB translocates to the nucleus to bind to DNA and upregulates the expression of inflammation-related genes [50]. However, RCAEA treatment substantially reversed this process by reducing I-κBα phosphorylation, indicating that its anti-inflammatory activity is closely associated with the NF-κB pathway.

Conversely, the NF-κB pathway can be inhibited by Nrf2/SKN-1 to alleviate the inflammatory response caused by oxidative stress. Both the NF-κB and SKN-1/Nrf2 pathways require transcriptional co-activators to initiate gene expression. Under oxidative stress, JNK and p38 MAPK can activate *skn-1.* When *skn-1* is activated, its enhanced binding to co-activators may reduce the availability of these cofactors for the NF-κB pathway, thereby suppressing the transcription of pro-inflammatory cytokines. In contrast, the activation of Nrf2/SKN-1 induces the expression of antioxidant enzymes, which collectively reduce intracellular ROS levels and indirectly suppress the activation of the NF-κB pathway. Akt-1 serves as a key upstream modulator that bridges these two signaling cascades [51–54]. Therefore, we verified this theory in *C. elegans*.

C. elegans is widely used for studying aging, longevity, and toxicology [55]. To assess the direct influence of RCAEA on *C. elegans*, we employed two biological behaviors studied in *C. elegans* research: head wiggle and reproductive capacity [56]. Additionally, we selected several other indicators that can directly reflect the degree of aging. Lipofuscin, an oxidative by-product, serves as a classic biomarker of aging in *C. elegans*, as excessive accumulation accelerates the aging process [57]. Meanwhile, as age advances, ROS production surpasses the clearance capacity, disrupting redox balance and inducing oxidative stress, a major contributor to aging [58]. Related to these is stress resistance, a key indicator of an organism's ability to endure external challenges. And lifespan experiments directly evaluated the effect of RCAEA on lifespan [59,60]. Our data indicated that RCAEA enhanced the survival percentage and stress resistance of *C. elegans* by improving its antioxidant capacity.

Furthermore, we detected gene expression levels of *src-1*, *let-23*, *trf-2*, and *akt-1* according to the predictions by network pharmacology, which are the direct homologs of SRC, EGFR, TRAFs, and AKT-1, respectively. *src-1* is a crucial kinase linked to NF-κB p65 and MAPKs, and it is associated with aging [61,62]. *let-23* acts upstream of the MAPK and phosphoinositide signaling pathways [63]. *let-23* activation reduces age-related pigment accumulation and influences mobility in advanced age [64]. *trf-2* is a homolog of human TRAFs. TRAF proteins interact with p38 MAPK and NF-κB, influencing cell survival and death [65]. *akt* (protein kinase B) plays a central role in the insulin signaling pathway, with impairment of this pathway extending *C. elegans'* longevity [66]. These genes are crucial in aging. RCAEA exerts an influence on these genes, suggesting that it may modulate them via the p38 MAPK/PMK-1 pathway.

Notably, the activity of *skn-1* is regulated by the p38 MAPK/PMK-1 signaling pathway. *skn-1* belongs to the NRF/CNC protein family, shares homology with NRF2, and plays an important role in *C. elegans* [67,68]. *pmk-1* activation facilitates *skn-1* nuclear translocation, enhancing cellular oxidative stress resistance by upregulating antioxidant genes such as *gst-4* [69]. *skn-1* primarily targets *sod-1* and *sod-3* in the SOD gene family, which directly regulate ROS levels [70]. Hence, the absence of *skn-1*, *sek-1*, and *pmk-1* may prevent RCAEA from extending the lifespan of these mutants or enhancing their anti-stress resistance [71]. Our speculation has been confirmed.

Previous studies have revealed that caudatin is a C_{21} steroidal glycoside derived from the root of *Cynanchum auriculatum*, which shows attenuating inflammatory effects by inhibiting PI3K/AKT and NF-κB signaling pathways [72,73]. As the most abundant phytosterol, β-Sitosterol plays a role in modulating the inflammatory response [74,75].

β-Sitosterol reduces Akt-1 phosphorylation, which in turn decreases IκBα phosphorylation and blocks the nuclear translocation of NF-κB. Meanwhile, it activates the Nrf2/SKN-1 signaling pathway to maintain redox balance [76–78]. 4-hydroxyacetophenone is effective against inflammation. It has also been demonstrated to be an antipigmentation reagent via inhibiting tyrosinase activity [79]. Baishouwubenzophenone has anti-functional dyspepsia effects [80]. These independent findings strongly corroborate our bioinformatic analysis, suggesting that the anti-aging effects of RCAEA are likely mediated through these precise compound–target interactions. While this cross-validation with published data significantly strengthens our hypothesis, future work will focus on the direct experimental verification of these interactions.

This study has demonstrated that RCAEA possesses potent anti-inflammatory and anti-aging properties. We discovered that RCAEA suppresses LPS-induced M1 macrophage polarization by inhibiting the NF-κB signaling pathway and extends the lifespan of *C. elegans* via regulating the PMK-1/SKN-1 pathway. These findings significantly advance our understanding of the pharmacological mechanisms of a traditional herb, positioning RCAEA as a promising multi-target agent that links the control of chronic inflammation to the promotion of longevity. This work provides a scientific foundation for the development of RCAEA or its active components into nutraceuticals or therapeutics for age-related inflammatory diseases.

Our research has certain limitations. *C. elegans* is the primary in vivo model used, which, although powerful for initial screening, necessitates validation in more complex mammalian systems. The predictive accuracy of network pharmacology may be affected by several factors, such as interspecies differences. Therefore, verifying network pharmacology predictions with experiments will help clarify the mechanism underlying the observed pharmacological effects. Furthermore, the specific compounds within RCAEA responsible for the observed effects have not been isolated and fully characterized. Future research should focus on identifying the key bioactive molecules in RCAEA and evaluating their efficacy in murine models of aging and inflammation.

In summary, our work not only elucidates a novel mechanism of action for RCAEA but also opens up new avenues for combating aging and its associated inflammatory pathologies.

5. Conclusions

This study assessed the impacts of RCAEA on inflammation regulation and aging in RAW264.7 cells and *C. elegans* and demonstrated that RCAEA inhibits LPS-induced M1 polarization in RAW264.7 macrophages and suppresses inflammatory responses by modulating NF-κB signaling pathways. Importantly, RCAEA enhanced stress resistance, mitigated oxidative damage, and prolonged the lifespan through the regulation of the PMK-1/SKN-1 signaling pathway, all without adverse effects on reproduction, underscoring its potential as a promising candidate for future development into a dietary supplement or a pharmaceutical agent. Overall, this study establishes the groundwork for the practical application of RCAEA.

Supplementary Materials: The supporting information can be downloaded at: https://www.mdpi.com/article/10.3390/cimb47110934/s1.

Author Contributions: Conceptualization, J.F.; methodology, J.F.; formal analysis, J.F.; investigation, J.F., Y.S., and Y.X.; resources, J.Y., J.R. and K.H.; writing—original draft preparation, J.F. and Y.S.; writing—review and editing, J.F. and Y.S.; visualization, J.F.; supervision, J.R.; project administration, J.R. and K.H.; funding acquisition, J.R. and K.H. All authors have read and agreed to the published version of the manuscript.

Funding: This research received no external funding.

Institutional Review Board Statement: Not applicable.

Informed Consent Statement: Not applicable.

Data Availability Statement: The original contributions presented in this study are included in the article/Supplementary Materials. Further inquiries can be directed to the corresponding author(s).

Conflicts of Interest: The authors declare no conflicts of interest.

Abbreviations

Akt, protein kinase B; BP, biological process; CA, *Cynanchum auriculatum* Royle ex Wight.; *C. elegans*, *Caenorhabditis elegans*; CGC, Caenorhabditis Genetics Center; CC, cellular component; COX-2, Cyclooxygenase-2; DCF-DA, 2′,7′-Dichlorofluorescein Diacetate; DMEM, Dulbecco's Modified Eagle Medium; DNA, deoxyribonucleic acid; *E. coli* OP50, *Escherichia coli* OP50; ELISA, Enzyme-Linked Immunosorbent Assay; GO, Gene Ontology; IL-1β, interleukin-1β; IL-6, interleukin-6; KEGG, Kyoto Encyclopedia of Genes and Genomes; LPS, lipopolysaccharide; LC-MS/MS, liquid chromatography–tandem mass spectrometry; MTT, methyl thiazolyl tetrazolium; MAPK, mitogen-activated protein kinase; MF, molecular function; NGM, nematode growth medium; NP, network pharmacology; NO, nitric oxide; iNOS, inducible nitric oxide synthase; NF-κB, nuclear factor kappa-B; PPI, protein–protein interaction; PGE2, prostaglandin E2; RIPA, radio immunoprecipitation assay; RCA, *Cynanchi Auriculati Radix*; RCAEA, the ethyl acetate extract of RCA; ROS, reactive oxygen species; qRT-PCR, real-time quantitative PCR assay; NaN_3, sodium azide; TCMSP, Traditional Chinese Medicine Systems Pharmacology; TNF-α, tumor necrosis factor-α.

References

1. Meccariello, R.; D'angelo, S. Impact of Polyphenolic-Food on Longevity: An Elixir of Life. An Overview. *Antioxidants* **2021**, *10*, 507. [CrossRef]
2. Hajam, Y.A.; Rani, R.; Ganie, S.Y.; Sheikh, T.A.; Javaid, D.; Qadri, S.S.; Pramodh, S.; Alsulimani, A.; Alkhanani, M.F.; Harakeh, S.; et al. Oxidative Stress in Human Pathology and Aging: Molecular Mechanisms and Perspectives. *Cells* **2022**, *11*, 552. [CrossRef]
3. Hong, M.; Yu, J.; Wang, X.; Liu, Y.; Zhan, S.; Wu, Z.; Zhang, X. Tea Polyphenols as Prospective Natural Attenuators of Brain Aging. *Nutrients* **2022**, *14*, 3012. [CrossRef]
4. Andonian, B.J.; Hippensteel, J.A.; Abuabara, K.; Boyle, E.M.; Colbert, J.F.; Devinney, M.J.; Faye, A.S.; Kochar, B.; Lee, J.; Litke, R.; et al. Inflammation and aging-related disease: A transdisciplinary inflammaging framework. *GeroScience* **2024**, *47*, 515–542. [CrossRef]
5. Singh, A.; Schurman, S.H.; Bektas, A.; Kaileh, M.; Roy, R.; Wilson, D.M.; Sen, R.; Ferrucci, L. Aging and Inflammation. *Cold Spring Harb. Perspect. Med.* **2024**, *14*, a041197. [CrossRef]
6. Pan, W.; Li, W.; Wu, H.; Xie, X.; Xie, M.; Nie, Q.; Liu, Z.; Cai, S. Aging-Accelerated Mouse Prone 8 (SAMP8) Mice Experiment and Network Pharmacological Analysis of Aged Liupao Tea Aqueous Extract in Delaying the Decline Changes of the Body. *Antioxidants* **2023**, *12*, 685. [CrossRef]
7. Ma, J.; Zhang, H.; Wang, Z.; Xu, C.; Tan, H.; Sun, Y.; Zheng, R.; Jin, Z.; Li, Y.; Ge, X.; et al. *Lycopodium japonicum* Thunb. inhibits chondrocyte apoptosis, senescence and inflammation in osteoarthritis through STING/NF-κB signaling pathway. *J. Ethnopharmacol.* **2024**, *335*, 118660. [CrossRef]
8. Yang, D.; Namila; Hashentuya; Tana; Wuyunsiqin; Zhao, W.; Menggenduxi; Wang, M. Mongolian medicine Qiqirigan-8 inhibition of PI3K/AKT/mTOR signaling pathway activation to ameliorate non-alcoholic Steatohepatitis. *J. Pharm. Biomed. Anal.* **2025**, *265*, 116975. [CrossRef] [PubMed]
9. Zhao, L.; Zhang, H.; Li, N.; Chen, J.; Xu, H.; Wang, Y.; Liang, Q. Network pharmacology, a promising approach to reveal the pharmacology mechanism of Chinese medicine formula. *J. Ethnopharmacol.* **2023**, *309*, 116306. [CrossRef] [PubMed]
10. Pan, H.T.; Xi, Z.Q.; Wei, X.Q.; Wang, K. A network pharmacology approach to predict potential targets and mechanisms of "*Ramulus cinnamomi* (cassiae)—*Paeonia lactiflora*" herb pair in the treatment of chronic pain with comorbid anxiety and depression. *Ann. Med.* **2022**, *54*, 413–425. [CrossRef] [PubMed]
11. Xu, J.; Bai, C.; Huang, L.; Liu, T.; Wan, Y.; Zheng, Z.; Ma, X.; Gao, F.; Yu, H.; Gu, X. Network pharmacology to dissect the mechanisms of Yinlai Decoction for pneumonia. *BMC Complement. Med. Ther.* **2020**, *20*, 168. [CrossRef]
12. Zhou, A.; Li, X.; Zou, J.; Wu, L.; Cheng, B.; Wang, J. Discovery of potential quality markers of Fritillariae thunbergii bulbus in pneumonia by combining UPLC-QTOF-MS, network pharmacology, and molecular docking. *Mol. Divers.* **2023**, *28*, 787–804. [CrossRef]

13. Wang, L.; Cai, F.; Zhao, W.; Tian, J.; Kong, D.; Sun, X.; Liu, Q.; Chen, Y.; An, Y.; Wang, F.; et al. *Cynanchum auriculatum* Royle ex Wight., *Cynanchum bungei* Decne. and *Cynanchum wilfordii* (Maxim.) Hemsl.: Current Research and Prospects. *Molecules* **2021**, *26*, 7065. [CrossRef]
14. Zhang, X.; Gao, M.; Rao, Z.; Lei, Z.; Zeng, J.; Huang, Z.; Shen, C.; Zeng, N. The antitumour activity of C21 steroidal glycosides and their derivatives of Baishouwu: A review. *J. Ethnopharmacol.* **2022**, *293*, 115300. [CrossRef] [PubMed]
15. Wu, Z.; Wang, Y.; Meng, X.; Wang, X.; Li, Z.; Qian, S.; Wei, Y.; Shu, L.; Ding, Y.; Wang, P.; et al. Total C-21 steroidal glycosides, isolated from the root tuber of *Cynanchum auriculatum* Royle ex Wight, attenuate hydrogen peroxide-induced oxidative injury and inflammation in L02 cells. *Int. J. Mol. Med.* **2018**, *42*, 3157–3170. [CrossRef]
16. Li, S.; Sun, Y.; Peng, H.; You, R.; Bai, F.; Chen, D.; Abdin, M.; Peng, C.; Li, X.; Cai, H.; et al. Chemical Composition of *Cynanchum auriculatum* Royle Ex Wight and Its Potential Role in Ameliorating Colitis. *Food Sci. Nutr.* **2025**, *13*, e4764. [CrossRef] [PubMed]
17. Zhang, J.; Chen, L.; Zhao, C.; Chen, Z.; Xiao, S.; Yin, X.; Wu, N.; Yang, L.; Xu, J.; Zhou, H.; et al. Polysaccharides from *Cynanchum auriculatum* Royle ex Wight ameliorate symptoms of hyperglycemia by regulating gut microbiota in type 2 diabetes mellitus mice. *Int. J. Biol. Macromol.* **2025**, *299*, 139878, Erratum in *Int. J. Biol. Macromol.* **2025**, *303*, 140624. [CrossRef]
18. Ren, J.; Su, Y.; Zeng, L.; Zhou, J.; Yi, S.; Xing, Y.; Kun, H. Ethyl Acetate Extract of *Radix Cynanchi Auriculati* Exerts Antioxidant Effects on LPS-induced RAW264.7 Cells by Regulating MAPKs/Nrf2/HO-1 Pathways. *Acad. J. Sci. Technol.* **2023**, *5*, 144–148. [CrossRef]
19. Yang, L.; Zheng, C.; Xia, Y.-F.; Dai, Y.; Wei, Z.-F. 3, 3′-diindolylmethane enhances macrophage efferocytosis and subsequently relieves visceral pain via the AhR/Nrf2/Arg-1-mediated arginine metabolism pathway. *Phytomedicine* **2023**, *116*, 154874. [CrossRef]
20. Ren, J.; Su, D.; Li, L.; Cai, H.; Zhang, M.; Zhai, J.; Li, M.; Wu, X.; Hu, K. Anti-inflammatory effects of Aureusidin in LPS-stimulated RAW264.7 macrophages via suppressing NF-κB and activating ROS- and MAPKs-dependent Nrf2/HO-1 signaling pathways. *Toxicol. Appl. Pharmacol.* **2020**, *387*, 114846. [CrossRef]
21. Xuan, A.; Liu, M.; Zhang, L.; Lu, G.; Liu, H.; Zheng, L.; Shen, J.; Zou, Y.; Zhi, S. SZC-6 Promotes Diabetic Wound Healing in Mice by Modulating the M1/M2 Macrophage Ratio and Inhibiting the MyD88/NF-χB Pathway. *Pharmaceuticals* **2025**, *18*, 1143. [CrossRef] [PubMed]
22. Wu, S.; Miao, J.; Zhu, S.; Wu, X.; Shi, J.; Zhou, J.; Xing, Y.; Hu, K.; Ren, J.; Yang, H. Pongamol Prevents Neurotoxicity via the Activation of MAPKs/Nrf2 Signaling Pathway in H_2O_2-Induced Neuronal PC12 Cells and Prolongs the Lifespan of *Caenorhabditis elegans*. *Mol. Neurobiol.* **2024**, *61*, 8219–8233. [CrossRef]
23. Wu, X.; Su, D.; Xu, J.; Ge, G.; Zhang, Y.; Wu, B.; Hu, K.; Ren, J.; Yang, H. Tricetin, a Dietary Flavonoid, Alleviates Neuroinflammation and Promotes Autophagy in Alzheimer's Disease by Regulating the PI3K/Akt/mTOR Signaling Pathway. *J. Agric. Food Chem.* **2025**, *73*, 9677–9689. [CrossRef]
24. Wang, G.; Song, B.; Jia, X.; Yin, H.; Li, R.; Liu, X.; Chen, J.; Zhang, J.; Wang, Z.; Zhong, S. Ceramides from Sea Red Rice Bran Improve Health Indicators and Increase Stress Resistance of *Caenorhabditis elegans* through Insulin/IGF-1 Signaling (IIS) Pathway and JNK-1. *J. Agric. Food Chem.* **2022**, *70*, 15080–15094. [CrossRef]
25. Ückert, A.K.; Rütschlin, S.; Gutbier, S.; Wörz, N.C.; Miah, M.R.; Martins, A.C.; Hauer, I.; Holzer, A.-K.; Meyburg, B.; Mix, A.K.; et al. Identification of the bacterial metabolite aerugine as potential trigger of human dopaminergic neurodegeneration. *Environ. Int.* **2023**, *180*, 108229. [CrossRef]
26. Guo, X.; Xin, Q.; Wei, P.; Hua, Y.; Zhang, Y.; Su, Z.; She, G.; Yuan, R. Antioxidant and anti-aging activities of Longan crude and purified polysaccharide (LP-A) in nematode *Caenorhabditis elegans*. *Int. J. Biol. Macromol.* **2024**, *267*, 131634. [CrossRef] [PubMed]
27. Gao, X.; Yu, J.; Li, Y.; Shi, H.; Zhang, L.; Fang, M.; Liu, Y.; Huang, C.; Fan, S. 27-Hydroxymangiferolic Acid Extends Lifespan and Improves Neurodegeneration in *Caenorhabditis elegans* by Activating Nuclear Receptors. *Molecules* **2025**, *30*, 1010. [CrossRef]
28. Shang, Y.; Chen, K.; Ni, H.; Zhu, X.; Yuan, X.; Wang, Y.; Liu, X.; Cui, Z.; Niu, Y.; Shi, Y.; et al. Environmentally relevant concentrations of perfluorobutane sulfonate impair locomotion behaviors and healthspan by downregulating mitophagy in *C. elegans*. *J. Hazard. Mater.* **2024**, *480*, 135938. [CrossRef]
29. Bei, Y.; Wang, T.; Guan, S. Berberine Extends Lifespan in *C. elegans* Through Multi-Target Synergistic Antioxidant Effects. *Antioxidants* **2025**, *14*, 450. [CrossRef] [PubMed]
30. Hu, K.; Wu, S.; Xu, J.; Zhang, Y.; Zhang, Y.; Wu, X.; Miao, J.; Yao, Y.; Zhu, S.; Chen, G.; et al. Pongamol Alleviates Neuroinflammation and Promotes Autophagy in Alzheimer's Disease by Regulating the Akt/mTOR Signaling Pathway. *J. Agric. Food Chem.* **2024**, *72*, 13634–13645. [CrossRef]
31. Chen, H.; Hu, Q.; Wen, T.; Luo, L.; Liu, L.; Wang, L.; Shen, X. Arteannuin B, a sesquiterpene lactone from Artemisia annua, attenuates inflammatory response by inhibiting the ubiquitin-conjugating enzyme UBE2D3-mediated NF-κB activation. *Phytomedicine* **2024**, *124*, 155263. [CrossRef] [PubMed]
32. Raish, M.; Ahmad, A.; Ansari, M.A.; Alkharfy, K.M.; Aljenoobi, F.I.; Jan, B.L.; Al-Mohizea, A.M.; Khan, A.; Ali, N. Momordica charantia polysaccharides ameliorate oxidative stress, inflammation, and apoptosis in ethanol-induced gastritis in mucosa through NF-kB signaling pathway inhibition. *Int. J. Biol. Macromol.* **2018**, *111*, 193–199. [CrossRef] [PubMed]

33. Zhao, W.; Ma, L.; Cai, C.; Gong, X. Caffeine Inhibits NLRP3 Inflammasome Activation by Suppressing MAPK/NF-κB and A2aR Signaling in LPS-Induced THP-1 Macrophages. *Int. J. Biol. Sci.* **2019**, *15*, 1571–1581. [CrossRef] [PubMed]
34. Wang, X.; Li, X.; Li, L.; Yang, X.; Wang, J.; Liu, X.; Chen, J.; Liu, S.; Zhang, N.; Li, J.; et al. Hawthorn fruit extract ameliorates H_2O_2-induced oxidative damage in neuronal PC12 cells and prolongs the lifespan of *Caenorhabditis elegans* via the IIS signaling pathway. *Food Funct.* **2022**, *13*, 10680–10694. [CrossRef] [PubMed]
35. Hua, X.; Feng, X.; Hua, Y.; Wang, D. Paeoniflorin attenuates polystyrene nanoparticle-induced reduction in reproductive capacity and increase in germline apoptosis through suppressing DNA damage checkpoints in *Caenorhabditis elegans*. *Sci. Total. Environ.* **2023**, *871*, 162189. [CrossRef]
36. Stillman, J.M.; Mendes Lopes, F.; Lin, J.P.; Hu, K.; Reich, D.S.; Schafer, D.P. Lipofuscin-like autofluorescence within microglia and its impact on studying microglial engulfment. *Nat. Commun.* **2023**, *14*, 7060. [CrossRef]
37. Ferreira, I.C.; Côrrea, R.C.D.; Orué, S.L.; Leite, D.F.; Da Rocha, P.D.S.; Cardoso, C.A.L.; Mussury, R.M.; Vit, P.; De Picoli Souza, K.; Dos Santos, E.L.; et al. Chemical Components and Antioxidant Activity of *Geotrigona* sp. and *Tetragonisca fiebrigi* Stingless Bee Cerumen Reduce Juglone-Induced Oxidative Stress in *Caenorhabditis elegans*. *Antioxidants* **2023**, *12*, 1276. [CrossRef]
38. Taylor, S.K.B.; Minhas, M.H.; Tong, J.; Selvaganapathy, P.R.; Mishra, R.K.; Gupta, B.P. *C. elegans* electrotaxis behavior is modulated by heat shock response and unfolded protein response signaling pathways. *Sci. Rep.* **2021**, *11*, 3115. [CrossRef]
39. Liu, F.; Wang, H.; Zhu, X.; Jiang, N.; Pan, F.; Song, C.; Yu, C.; Yu, C.; Qin, Y.; Hui, J.; et al. Sanguinarine promotes healthspan and innate immunity through a conserved mechanism of ROS-mediated PMK-1/SKN-1 activation. *iScience* **2022**, *25*, 103874. [CrossRef]
40. Tambara, A.L.; Silveira, É.C.; Soares, A.T.G.; Salgueiro, W.G.; Rodrigues, C.D.F.; Boldori, J.R.; Ávila, D.S.; Denardin, C.C. Butiá fruit extract (*Butia eriospatha*) protects against oxidative damage and increases lifespan on *Caenorhabditis elegans*. *J. Food Biochem.* **2020**, *44*, e13139. [CrossRef]
41. Petrovic, D.; Slade, L.; Paikopoulos, Y.; D'andrea, D.; Savic, N.; Stancic, A.; Miljkovic, J.L.; Vignane, T.; Drekolia, M.K.; Mladenovic, D.; et al. Ergothioneine improves healthspan of aged animals by enhancing cGPDH activity through CSE-dependent persulfidation. *Cell Metab.* **2025**, *37*, 789. [CrossRef]
42. Liu, M.; Li, N.; Shan, S.; Shi, Y.; Zhu, Y.; Lu, W. Acanthopanax senticosus Polysaccharide Enhances the Pathogen Resistance of Radiation-Damaged *Caenorhabditis elegans* through Intestinal p38 MAPK-SKN-1/ATF-7 Pathway and Stress Response. *Int. J. Mol. Sci.* **2022**, *23*, 5034. [CrossRef]
43. Matilainen, O.; Ribeiro, A.R.S.; Verbeeren, J.; Cetinbas, M.; Sood, H.; Sadreyev, R.I.; Garcia, S.M.D.A. Loss of muscleblind splicing factor shortens *Caenorhabditis elegans* lifespan by reducing the activity of p38 MAPK/PMK-1 and transcription factors ATF-7 and Nrf/SKN-1. *Genetics* **2021**, *219*, iyab114. [CrossRef]
44. Wen, J.H.; Li, D.Y.; Liang, S.; Yang, C.; Tang, J.X.; Liu, H.F. Macrophage autophagy in macrophage polarization, chronic inflammation and organ fibrosis. *Front. Immunol.* **2022**, *13*, 946832. [CrossRef] [PubMed]
45. Yang, T.; Qu, X.; Zhao, J.; Wang, X.; Wang, Q.; Dai, J.; Zhu, C.; Li, J.; Jiang, L. Macrophage PTEN controls STING-induced inflammation and necroptosis through NICD/NRF2 signaling in APAP-induced liver injury. *Cell Commun. Signal.* **2023**, *21*, 160. [CrossRef] [PubMed]
46. Zhan, Y.; Xu, D.; Tian, Y.; Qu, X.; Sheng, M.; Lin, Y.; Ke, M.; Jiang, L.; Xia, Q.; Kaldas, F.M.; et al. Novel role of macrophage TXNIP-mediated CYLD–NRF2–OASL1 axis in stress-induced liver inflammation and cell death. *JHEP Rep.* **2022**, *4*, 100532. [CrossRef]
47. Capece, D.; Verzella, D.; Flati, I.; Arboretto, P.; Cornice, J.; Franzoso, G. NF-κB: Blending metabolism, immunity, and inflammation. *Trends Immunol.* **2022**, *43*, 757–775. [CrossRef]
48. Xie, Z.; Lin, M.; Xing, B.; Wang, H.; Zhang, H.; Cai, Z.; Mei, X.; Zhu, Z.-J. Citrulline regulates macrophage metabolism and inflammation to counter aging in mice. *Sci. Adv.* **2025**, *11*, eads4957. [CrossRef] [PubMed]
49. Liu, M.; Guan, G.; Wang, Y.; Lu, X.; Duan, X.; Xu, X. p-Hydroxy benzaldehyde, a phenolic compound from Nostoc commune, ameliorates DSS-induced colitis against oxidative stress via the Nrf2/HO-1/NQO-1/NF-κB/AP-1 pathway. *Phytomedicine* **2024**, *133*, 155941. [CrossRef]
50. Wang, W.T.; Zhang, Y.Y.; Li, Z.R.; Li, J.M.; Deng, H.S.; Li, Y.Y.; Yang, H.Y.; Lau, C.C.; Yao, Y.J.; Pan, H.D.; et al. Syringic acid attenuates acute lung injury by modulating macrophage polarization in LPS-induced mice. *Phytomedicine* **2024**, *129*, 155591. [CrossRef]
51. Zhao, X.; Duan, B.; Wu, J.; Huang, L.; Dai, S.; Ding, J.; Sun, M.; Lin, X.; Jiang, Y.; Sun, T.; et al. Bilirubin ameliorates osteoarthritis via activating Nrf2/HO-1 pathway and suppressing NF-κB signalling. *J. Cell. Mol. Med.* **2024**, *28*, e18173. [CrossRef]
52. Weng, J.; Chen, Z.; Weng, S.; Guo, R.; Shi, B.; Liu, D.; Huang, S. Study on the mechanism of action of Penehyclidine hydrochloride on LPS-induced acute lung injury by regulating autophagy through the mTOR/Keap1/Nrf2 signaling pathway. *J. Pharm. Biomed. Anal.* **2025**, *263*, 116938. [CrossRef]
53. Li, Q.; Liu, Y.; Dai, X.; Jiang, W.; Zhao, H. Nanozymes Regulate Redox Homeostasis in ROS-Related Inflammation. *Front. Chem.* **2021**, *9*, 740607. [CrossRef]

54. Zhang, Z.; Zhang, Y.; Cai, Y.; Li, D.; He, J.; Feng, Z.; Xu, Q. NAT10 regulates the LPS-induced inflammatory response via the NOX2-ROS-NF-κB pathway in macrophages. *Biochim. Biophys. Acta Mol. Cell Res.* **2023**, *1870*, 119521. [CrossRef]
55. De Freitas Rodrigues, C.; Ramos Boldori, J.; Valandro Soares, M.; Somacal, S.; Emanuelli, T.; Izaguirry, A.; Weber Santos Cibin, F.; Rossini Augusti, P.; Casagrande Denardin, C. Goji berry (*Lycium barbarum* L.) juice reduces lifespan and premature aging of Caenorhabditis elegans: Is it safe to consume it? *Food Res. Int.* **2021**, *144*, 110297. [CrossRef]
56. Yu, X.; Li, H.; Lin, D.; Guo, W.; Xu, Z.; Wang, L.; Guan, S. Ginsenoside Prolongs the Lifespan of *C. elegans* via Lipid Metabolism and Activating the Stress Response Signaling Pathway. *Int. J. Mol. Sci.* **2021**, *22*, 9668. [CrossRef]
57. Huang, Y.; Wang, Y.; Deng, J.; Gao, S.; Qiu, J.; He, J.; Yang, T.; Tan, N.; Cheng, S.; Song, Z. Research on the anti-oxidant and anti-aging effects of *Polygonatum kingianum* saponins in *Caenorhabditis elegans*. *Heliyon* **2024**, *10*, e35556. [CrossRef]
58. Sun, J.; Zhong, X.; Sun, D.; Xu, L.; Shi, L.; Sui, J.; Liu, Y. Anti-aging effects of polysaccharides from ginseng extract residues in *Caenorhabditis elegans*. *Int. J. Biol. Macromol.* **2023**, *225*, 1072–1084. [CrossRef] [PubMed]
59. Taylor, R.C.; Dillin, A. XBP-1 Is a Cell-Nonautonomous Regulator of Stress Resistance and Longevity. *Cell* **2013**, *153*, 1435–1447. [CrossRef] [PubMed]
60. Park, H.E.H.; Jung, Y.; Lee, S.J.V. Survival assays using *Caenorhabditis elegans*. *Mol. Cells* **2017**, *40*, 90–99. [CrossRef] [PubMed]
61. Ren, Q.; Guo, F.; Tao, S.; Huang, R.; Ma, L.; Fu, P. Flavonoid fisetin alleviates kidney inflammation and apoptosis via inhibiting Src-mediated NF-κB p65 and MAPK signaling pathways in septic AKI mice. *Biomed. Pharmacother.* **2020**, *122*, 109772. [CrossRef]
62. Xiao, X.; Xu, M.; Yu, H.; Wang, L.; Li, X.; Rak, J.; Wang, S.; Zhao, R.C. Mesenchymal stem cell-derived small extracellular vesicles mitigate oxidative stress-induced senescence in endothelial cells via regulation of miR-146a/Src. *Signal Transduct. Target. Ther.* **2021**, *6*, 354, Erratum in *Signal Transduct. Target. Ther.* **2022**, *7*, 234. [CrossRef] [PubMed]
63. Schwartz, H.T.; Sternberg, P.W. A sequencing-based screening method identifies regulators of EGFR signaling from nonviable mutants in *Caenorhabditis elegans*. *Sci. Signal.* **2025**, *18*, eadp9377. [CrossRef] [PubMed]
64. Detienne, G.; De Haes, W.; Ernst, U.R.; Schoofs, L.; Temmerman, L. Royalactin extends lifespan of *Caenorhabditis elegans* through epidermal growth factor signaling. *Exp. Gerontol.* **2014**, *60*, 129–135. [CrossRef] [PubMed]
65. Wajant, H.; Grell, M.; Scheurich, P. TNF receptor associated factors in cytokine signaling. *Cytokine Growth Factor Rev.* **1999**, *10*, 15–26. [CrossRef]
66. Li, W.; Chen, S.; Lang, J.; Luo, J.; Chen, J.; Zhang, L.; Sun, Z.; Dong, D. The clinical antiprotozoal drug nitazoxanide and its metabolite tizoxanide extend *Caenorhabditis elegans* lifespan and healthspan. *Acta Pharm. Sin. B* **2024**, *14*, 3266–3280. [CrossRef] [PubMed]
67. Li, R.; Yi, Q.; Wang, J.; Miao, Y.; Chen, Q.; Xu, Y.; Tao, M. Paeonol promotes longevity and fitness in *Caenorhabditis elegans* through activating the DAF-16/FOXO and SKN-1/Nrf2 transcription factors. *Biomed. Pharmacother.* **2024**, *173*, 116368. [CrossRef]
68. Jattujan, P.; Srisirirung, S.; Watcharaporn, W.; Chumphoochai, K.; Kraokaew, P.; Sanguanphun, T.; Prasertsuksri, P.; Thongdechsri, S.; Sobhon, P.; Meemon, K. 2-Butoxytetrahydrofuran and Palmitic Acid from Holothuria scabra Enhance *C. elegans* Lifespan and Healthspan via DAF-16/FOXO and SKN-1/NRF2 Signaling Pathways. *Pharmaceuticals* **2022**, *15*, 1374. [CrossRef]
69. Francisco, M.; Grau, R. Biofilm proficient Bacillus subtilis prevents neurodegeneration in *Caenorhabditis elegans* Parkinson's disease models via PMK-1/p38 MAPK and SKN-1/Nrf2 signaling. *Sci. Rep.* **2025**, *15*, 9864. [CrossRef]
70. Li, H.; Su, L.; Su, X.; Liu, X.; Wang, D.; Li, H.; Ba, X.; Zhang, Y.; Lu, J.; Huang, B.; et al. Arginine methylation of SKN-1 promotes oxidative stress resistance in *Caenorhabditis elegans*. *Redox Biol.* **2019**, *21*, 101111. [CrossRef]
71. Falcicchia, C.; Tozzi, F.; Arancio, O.; Watterson, D.M.; Origlia, N. Involvement of p38 MAPK in Synaptic Function and Dysfunction. *Int. J. Mol. Sci.* **2020**, *21*, 5624. [CrossRef]
72. Shi, G.; Ni, L.; Kong, X.; Ren, R.; Shi, X.; Xu, Y.; Qu, Z.; Zhou, H.; Zhang, X. Unveiling the therapeutic potential of caudatin: Structural optimization, pharmacological mechanisms, and therapeutic implications. *Front. Pharmacol.* **2025**, *16*, 1640365. [CrossRef] [PubMed]
73. Hou, J.; Chen, Q.; Huang, Y.; Wu, Z.; Ma, D. Caudatin blocks the proliferation, stemness and glycolysis of non-small cell lung cancer cells through the Raf/MEK/ERK pathway. *Pharm. Biol.* **2022**, *60*, 764–773. [CrossRef] [PubMed]
74. Wang, H.; Wang, Z.; Zhang, Z.; Liu, J.; Hong, L. β-Sitosterol as a Promising Anticancer Agent for Chemoprevention and Chemotherapy: Mechanisms of Action and Future Prospects. *Adv. Nutr.* **2023**, *14*, 1085–1110. [CrossRef] [PubMed]
75. Khan, Z.; Nath, N.; Rauf, A.; Emran, T.B.; Mitra, S.; Islam, F.; Chandran, D.; Barua, J.; Khandaker, M.U.; Idris, A.M.; et al. Multifunctional roles and pharmacological potential of β-sitosterol: Emerging evidence toward clinical applications. *Chem. Biol. Interact.* **2022**, *365*, 110117. [CrossRef]
76. Cao, W.; Yuan, F.; Liu, T.; Yin, R. Network pharmacology analysis, molecular docking integrated experimental verification reveal β-sitosterol as the active anti-NSCLC ingredient of *Polygonatum cyrtonema* Hua by suppression of PI3K/Akt/HIF-1α signaling pathway. *J. Ethnopharmacol.* **2024**, *328*, 117900. [CrossRef] [PubMed]
77. Wang, H.; Liu, J.; Zhang, Z.; Peng, J.; Wang, Z.; Yang, L.; Wang, X.; Hu, S.; Hong, L. β-Sitosterol targets ASS1 for Nrf2 ubiquitin-dependent degradation, inducing ROS-mediated apoptosis via the PTEN/PI3K/AKT signaling pathway in ovarian cancer. *Free Radic. Biol. Med.* **2024**, *214*, 137–157. [CrossRef]

78. Wang, X.; Mao, J. Systematic pharmacology-based strategy to investigate the mechanism of beta-sitosterol for the treatment of rheumarthritis. *Front. Genet.* **2024**, *15*, 1507606. [CrossRef]
79. Guo, Q.; Zhang, Y.; Tang, C.; Li, Q.; Liu, F.; He, Z.; Jiang, C.; Xu, J.; Zhao, H. 4-Hydroxyacetophenone is an Antipigmentation Reagent via Inhibiting Tryrosinase Activity. *ACS Omega* **2025**, *10*, 34811–34821. [CrossRef]
80. Sun, J.; Gou, J.; Qin, L.; Liu, T.; Huang, Y.; Lu, Y.; Wang, Y.; Liu, C.; Li, Y. Screening of anti-functional dyspepsia compounds in *Cynanchum auriculatum*: A spectrum-effect relationship analysis, and ATP-binding cassette transporters inhibitor evaluation. *J. Ethnopharmacol.* **2024**, *318*, 116867. [CrossRef]

Disclaimer/Publisher's Note: The statements, opinions and data contained in all publications are solely those of the individual author(s) and contributor(s) and not of MDPI and/or the editor(s). MDPI and/or the editor(s) disclaim responsibility for any injury to people or property resulting from any ideas, methods, instructions or products referred to in the content.